Research Article

A "Local First" Approach to Glacigenic Sediment Provenance Demonstrated Using U-Pb Detrital Zircon Geochronology of the Permo-Carboniferous Wynyard Formation, Tasmanian Basin

Libby R. W. Ives[1][a], John L. Isbell[1], Kathy J. Licht[2]

[1] Department of Geosciences, University of Wisconsin – Milwaukee, [2] Department of Earth Sciences, Indiana University-Purdue University Indianapolis

The Sedimentary Record

We propose that a "local first" approach should be applied to the interpretation of provenance indicators in glacigenic sediments of all depositional ages, especially where the glacier flow path is poorly constrained and the records of potential source lithologies are incomplete. Provenance proxies, specifically U-Pb detrital zircon geochronology, of glacigenic sediments are commonly used to infer the size and distribution of past ice centers, which are in turn used to inform ancient climate reconstructions. Interpretations of these proxies often assume that similar provenance signals between glacigenic units of the same depositional age are evidence that they were deposited by the same glacier, even when those units are, not infrequently, separated by thousands of kilometers. Though glaciers are capable of transporting sediment great distances, this assumption is problematic as it does not acknowledge observations from the geologic records of Pleistocene ice sheets that show provenance proxies in glacial sediments are most likely to reflect proximal (within 100 km) sediment sources located along a specific flow path. In a "local first" approach, provenance indicators are first compared to local source lithologies. If the indicator cannot be attributed to proximal sources, only then should progressively more distal sources be investigated. Applying a local first approach to sediment provenance in ancient glacial systems may result in significant revisions to paleo ice sheet reconstructions. The effectiveness of the local first approach is demonstrated here by comparing new U-Pb detrital zircon dates from the Permo-Carboniferous glacigenic Wynyard Fm with progressively distal source lithologies along the glacier's inferred flow path. The Wynyard Fm and source lithologies were compared using an inverse Monte-Carlo unmixing model (DZMix). All measured Wynyard Fm detrital zircon dates can be attributed to zircon sources within 33 km of the sample location along the glacier's flow path. This interpretation of a proximal detrital zircon provenance does not conflict with the popular interpretation made from sedimentological observations that the Wynyard Fm was deposited by a large, temperate outlet glacier or ice stream that flowed south-to-north across western Tasmania. Overall, a local first approach to glacial sediment provenance, though more challenging than direct comparisons between glacigenic sedimentary deposits, has the potential to elucidate the complex histories and flow paths of glacial sedimentary systems of all depositional ages.

Introduction

Constraining the provenance of glacigenic sediments from past ice ages is a key tool in determining the size and distribution of ancient ice centers (e.g., Griffis et al., 2019; Martin et al., 2019; Zurli et al., 2022). The inferred characteristics of these ice centers are lynchpins in understanding climate through geologic time, including the Late Paleozoic Ice Age (LPIA; Isbell et al., 2012). Recent publications have attempted to reconstruct Paleozoic ice sheet distributions

[a] Corresponding author:
libby.r.w.ives@gmail.com

using detrital zircon (DZ) U-Pb geochronology, including some studies that inferred continent-scale glacial sediment transport systems during the Paleozoic (e.g., Craddock et al., 2019; Griffis et al., 2019). These works often assume that similar DZ provenance signals between geographically dispersed glacigenic sediments of equivalent depositional age are evidence that they were deposited by the same large mass (i.e., an ice sheet, ice cap, or outlet glacier).

This assumption is not physically reasonable for glacial transport systems for largely two reasons. First, large ice masses generally radiate out from one or more central domes, thus flow is not uni-directional (e.g., Andrews & Fulton, 1987). Accordingly, glaciers cannot carry sediment from one edge of an ice sheet to another, as has been proposed in some models of LPIA provenance (e.g., Craddock et al., 2019). Radially divergent flow patterns cross many potential combinations of source rocks within the footprint of a large ice mass, and sediments deposited by different parts of the same ice mass may not have similar provenance signals (Licht & Hemming, 2017). Second, the unique ways in which glaciers entrain, transport, and deposit sediments differ significantly from other sedimentary transport systems, such as continent-scale fluvial drainages (e.g., Lawton et al., 2021). Glacial processes are more likely to create and deposit sediments dominated by proximal sources than sources greater than 1000 km up-glacier because the relative abundance of a subglacially entrained sediment decreases exponentially downglacier from its source and is most likely to be detectable only within 100 km of a point-source (Clark, 1987; Hooke et al., 2013; Kujansuu & Saarnisto, 1990; Larson & Mooers, 2008; Salonen, 1986).

We propose that a "local" null hypothesis is the most appropriate way to approach interpretations of provenance indicators in glacigenic sediments, including DZ. Such an approach is especially useful in the ancient (pre-Pleistocene) record where glacier flow paths are poorly constrained, and millions of years of deposition and erosion of intermediary sedimentary units means the rock record is incomplete. In this approach, provenance indicators should first be compared to potential bedrock and contemporaneously unlithified sediment sources along the glacier's proposed flow path (if known) adjacent to the target sample's location. If the provenance indicator cannot be attributed to sources within these spatial constraints, then progressively more distal sources may be considered. DZ geochronology is a good provenance indicator to use as a case study of this "local first" approach because DZ dates can more easily be attributed to specific lithologic sources than other geochemical or petrographic provenance indicators.

In this paper, we demonstrate the effectiveness of a local first approach by testing whether the DZ populations in sandstone samples collected from a Permo-Carboniferous glaciomarine succession in Tasmania (Wynyard Fm) could have been derived from local lithologies along the glacier's inferred flow path. Newly measured DZ dates from the Wynyard Fm (N = 2, n = 592) were compared to DZ dates from pre-Permian western Tasmanian lithologies (N = 76, n = 2710) using an inverse Monte Carlo unmixing model

(DZMix; Sundell & Saylor, 2017). DZ date populations in sedimentary rocks can be used to identify the primary source lithology (i.e., igneous or metamorphic) of a certain date population (e.g., Mulder et al., 2015), or identify intermediate, sedimentary source lithologies through which certain zircon populations have been recycled (e.g., Andersen et al., 2016; Zotto et al., 2020). In this study, we aimed to identify the DZ source lithologies from which the "Wynyard glacier" (that is, the portion of a larger ice sheet that flowed through the Dundas Trough and deposited the Wynyard Fm) would have sourced sediments that were deposited as the Wynyard Fm, including both primary and intermediate zircon sources.

Geologic Context

The Permo-Carboniferous Wynyard Fm (also known as the "Wynyard Tillite") and its correlates across Tasmania make up the basal strata of the Parmeener Supergroup in the Tasmanian Basin (Clarke & Forsyth, 1989; Reid et al., 2014). These successions are mostly confined to structural and paleotopographic lows within the Tasmanian Basin (Hand, 1993; Reid et al., 2014). The Wynyard Fm crops out at the northern edge of one of these lows known as the Dundas Trough (Fig. 1A). In addition to being a paleotopographic low, the Dundas Trough is a distinct structural element of the West Tasmanian Terrane with a unique pre-Permian geologic history (Fig. S3). The Dundas Trough extends across mainland Tasmania's western side from its southern to northern coasts, and paleo flow directions associated with the Wynyard Fm indicate that the glacier flowed north through it (Fig. 1A; Hand, 1993). The Wynyard glacier is thought to be a large, temperate outlet glacier or ice stream, which was likely connected to an ice center located to the paleogeographic south of the Tasmanian Basin (Fig. 1; Hand, 1993; Henry et al., 2012; Ives, 2021; Powell, 1990; Reid et al., 2014). Pleistocene analogs to the proposed Wynyard glacier are the ice streams that flowed through the Hudson Strait, Frobisher Bay, and Cumberland Sound off Baffin Island in the Canadian Arctic Archipelago (e.g., Andrews et al., 1985; Andrews & MacLean, 2003). These ice streams had a similar topographic setting, glaciological context, and spatial scale to the proposed Wynyard glacier.

The Wynyard Fm is an appropriate example with which to test the local first approach primarily because the sediments were deposited in an ice-proximal setting by an ice mass that was actively eroding and transporting sediment subglacially (Henry et al., 2012; Powell, 1990). The samples used in this study were deposited as part of sandy, sub-aqueous grounding-line fan systems (Fig. 2; Henry et al., 2012; Ives, 2021; Powell, 1990). These sediments would have been sourced directly from subglacial materials and deposited in a proglacial marine environment near the ice margin. This depositional environment ensures that the zircons tested in this study were transported subglacially (by the ice and/or subglacial drainage systems) directly before deposition (Powell, 1990). This inference is supported by evidence for subglacial transport interpreted from the shape and striae on Wynyard Fm pebbles (Banks, 1981),
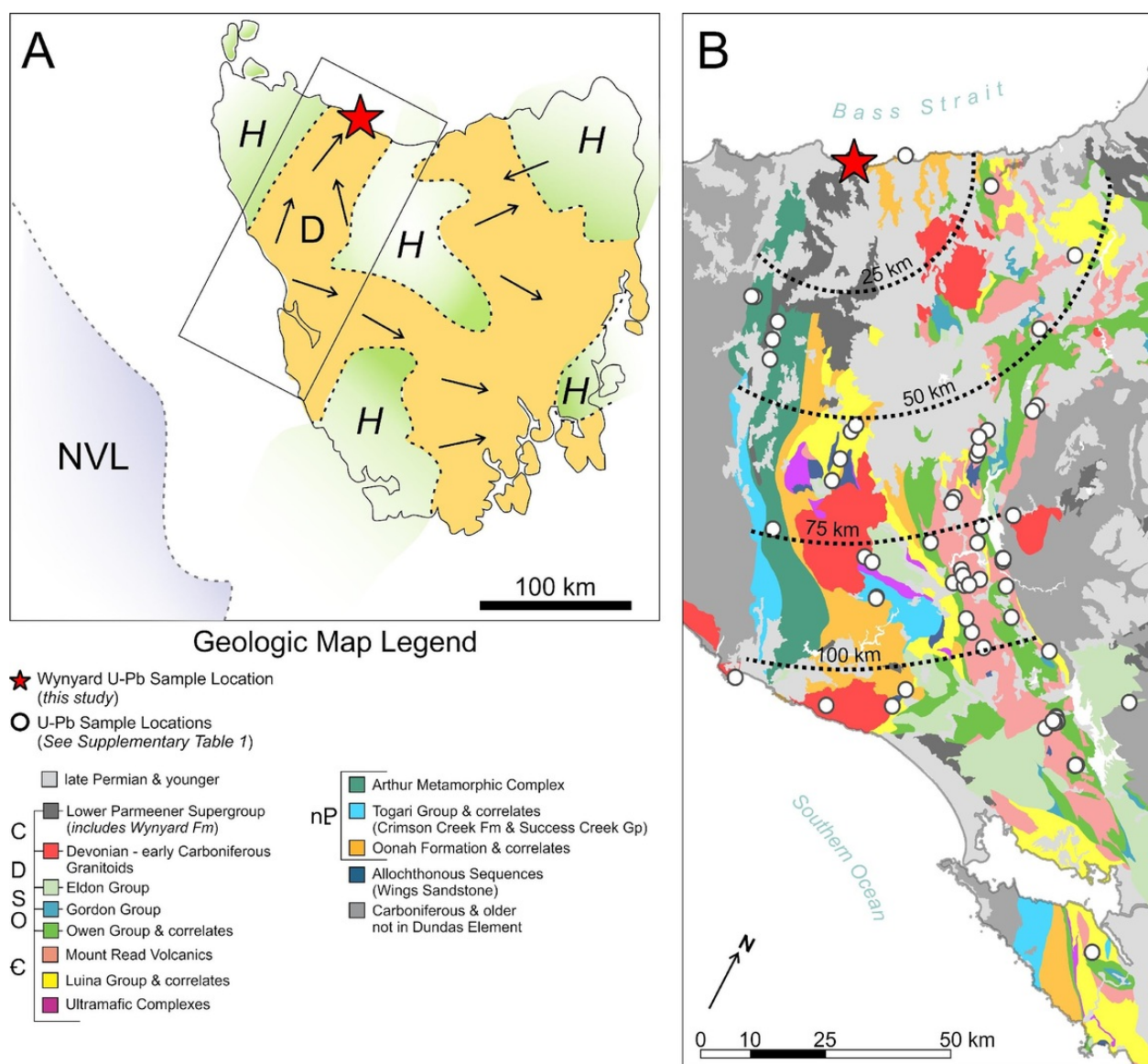
Figure 1. Geologic and paleogeographic context for the Wynyard Fm, Tasmania.

The red star on both maps shows the location where the Wynyard Fm samples were collected. **A.** Paleogeographic map of Tasmania during the deposition of the Wynyard Fm and correlates. Orange areas indicate the modern limits of the Wynyard Fm and correlates (both at the surface and in the subsurface) and are proposed paleotopographic lows. "D" notes the Dundas Trough. Areas labeled as "H" are paleotopographic highs. Arrows indicate ice paleoflow directions. The black box shows the extent of map 1B. The shaded area labeled NVL shows the approximate position of North Victoria Land during the late Carboniferous and early Permian, when the Wynyard Fm was deposited. Map and flow directions are after Hand (1993), Henry et al. (2012), Elliot (2013), and Reid et al. (2014). **B.** Geologic map of pre-Permian units in the Dundas Trough (Green et al., 2012). Dashed lines show distances from the Wynyard Fm site in 25 km intervals. White dots indicate the location of Dundas Trough potential source lithology samples with U-Pb zircon dates used in this study. Samples indicated by white dots that occur outside the footprint of the Dundas Trough were included in this study if there were limited or no detrital zircon records from that source lithology within the Trough.

cobbles, and boulders (Ives, 2021). Additionally, the paleo flow path of the Wynyard glacier is relatively well constrained (Hand, 1993; Fig. 1) and there are many "high-n" DZ data for source rocks along its proposed flow path (Fig 1.; Fig. 3; Fig. S3; File S1).

The provenance of the Wynyard Fm is not well characterized and identifying the source of these sediments may help clarify the distribution and size of ice centers during the LPIA. Based on flow directions, the Wynyard Fm is proposed to have been deposited by an ice mass centered in North Victoria Land (NVL), Antarctica, with contributions from ice masses located adjacent to the Dundas Trough (Fig. 1; Hand, 1993; Henry et al., 2012; Veevers, 2006; Zurli et al., 2022). Prior provenance work has demonstrated that

most Wynyard Fm clast lithologies are attributable to pre-Permian source rocks in western Tasmania (Banks, 1981; Hand, 1993), and not NVL sources.

Wynyard Fm zircon U-Pb measurements

Two moderately well-sorted, fine- to medium-grained sandstone samples were collected from the lower Wynyard Formation (n = 2; Fig. 2A). The composition of the sandstones are sub-lithic or lithic arenites (Henry et al., 2012; Ives, 2021). The samples were collected 75 m and 385 m above the Wynyard Fm's basal unconformity (Ives, 2021; Fig. S4; Fig. S5). Sample preparation (crushing, mineral separation, and grain mounting in epoxy pucks) was per-
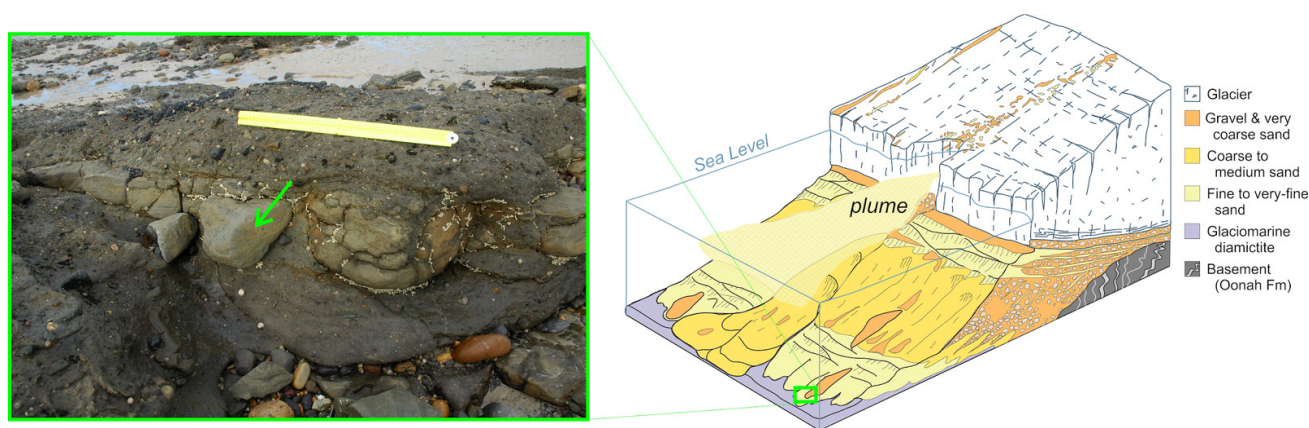
Figure 2. Depositional setting of Wynyard Fm sandstone samples.

A. Photograph of a fine-grained sandstone in Wynyard Fm, similar to the samples used for detrital zircon analysis in this study, indicated by the green arrow. The ruler in the photo is 0.5 m long. **B.** Diagram showing the proposed ice-contact depositional setting of the Wynyard Fm. These sandstones were most likely deposited from low density turbidity currents proximal to the ice margin as part of a morainal bank or grounding line fan (Henry et al., 2012; Ives, 2021). The green box indicates the approximate depositional setting of the sand body in A. Figure digitized from Lønne (1995).

formed by staff at the Arizona LaserChron Center at the University of Arizona (see methods in Gehrels (2000), Gehrels et al. (2008), and Gehrels and Pecha (2014)).

Zircons derived from the Wynyard Fm ranged in size from 50 – 180 μm (silt – fine sand) (N = 592). Grain imaging was performed with a backscatter electron detector system using a Hitachi S3400 scanning electron microscope to ensure analysis of zircon and to avoid inclusions and fractures. Cathodoluminescence images were also captured of grain mounts for qualitative assessment of mineral properties (Fig. S6). The U-Pb composition of 300 Wynyard Fm "unknown" grains were targeted and measured for each of the two samples. Grains were selected for measurement with the intention of creating a dataset from representative grain sizes. Spots were selected using Chromium Offline Targeting Software by Teledyne Photon Machine (version 2.4; File S5).

U–Pb isotopic analyses were conducted by LA-ICPMS using a Teledyne Photon Machines Analyte G2 laser connected to a Thermo Scientific Element 2 mass spectrometer (Pullen et al., 2018). Analyses utilized a 20 μm diameter laser beam fired at 7 Hz for 10s. FC-1 (Paces & Miller, 1993) and SL2 (Gehrels et al., 2008) were used as primary standards and R33 (Black et al., 2004) as a secondary standard (standards measurements and details reported in File S1). Three measurements of each FC-1 and SL2 were made prior to measuring any unknowns. Thereafter, a single standard measurement of alternating FC-1 and SL2 were made after every five unknowns. Every sixth primary standard measurement was accompanied by a measurement of standard R33. U–Pb dates, including common Pb corrections based on measured ^{204}Pb abundances, were calculated with E2AgeCalc (Gehrels et al., 2008; Pullen et al., 2018; File S2; File S3) and are reported in File S1. Default settings in the E2AgeCalc were used to filter data and select the "best age" for each measurement. For dates < 900 Ma, the $\frac{^{206}Pb}{^{238}U}$ ages were used and for dates > 900 Ma the $\frac{^{206}Pb}{^{207}Pb}$ ages were used. A relative age discordance filter was applied to dates >700

Ma. Discordance values are calculated as $\left(\frac{^{206}Pb/^{238}U}{^{206}Pb/^{207}Pb} \right) * 100$. Any analyses of Wynyard Fm zircon grains that were > 20% (positive value) discordant or > 5% reverse (negative value) discordant were not considered in the analyses made in this study (Pullen et al., 2018), though all measurements are reported in File S1. Concordia diagrams of Wynyard Fm measurements are shown in Figure S1.

The Wynyard Fm zircon dates range from 319 Ma to 3075 Ma (Fig. 3). The analyses from both samples were combined for this study because they have similar date populations that are not significant from one another when measurement uncertainties are accounted for (Fig. S2). The results of this study show a multimodal DZ date population in these Wynyard Fm sandstones with major age peaks at 375 Ma, 560 Ma, 1035 Ma, and 1785 Ma (Fig. 3). Some of these sub-populations can be easily attributed to specific geologic events and corresponding source lithologies. For example, dates in the Wynyard Fm population that make up the 375 Ma peak match zircon ages measured in Tasmanian granitoid intrusions that were emplaced as part of the Lachlan Orogen (Black et al., 2005, 2010; Hong et al. 2018; Fig. S3). However, most other sub-populations cannot be attributed to single source lithology or known geologic event. This complexity of the Wynyard Fm DZ date population motivated our use of a mixing model to determine whether this population could be made up of DZ contributed from bedrock along the Wynyard glacier's flow path.

Unmixing model

The relative proportion of Dundas Trough source lithologies contributing to the Wynyard Fm DZ were modeled using an inverse Monte Carlo approach (DZMix) (Sundell & Saylor, 2017). This approach used our new data from the Wynyard Fm and detrital zircon U-Pb dates for potential source lithologies in the Dundas Trough that were collected
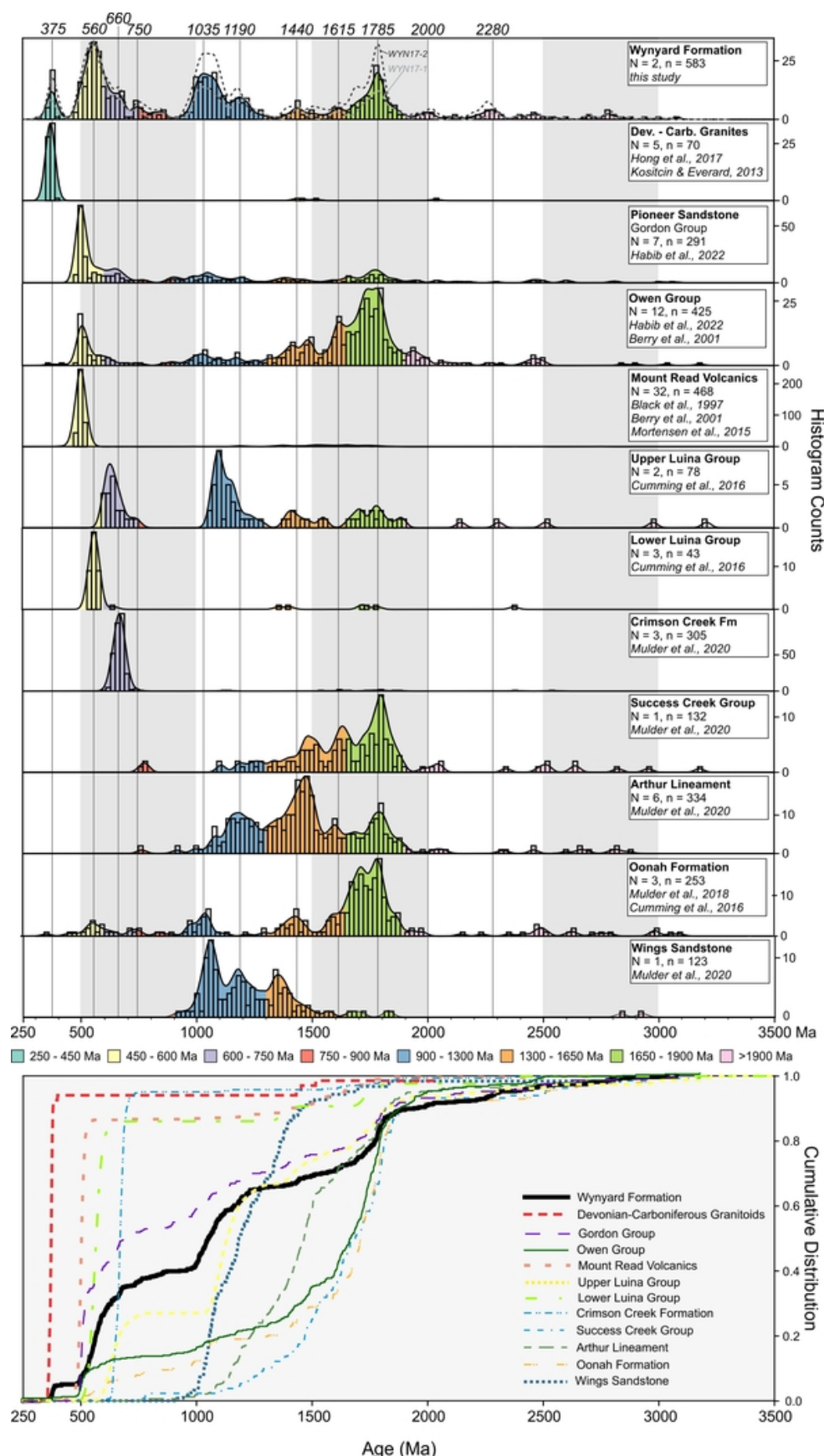
Figure 3. Relative and cumulative distributions of detrital zircon U-Pb dates for the Wynyard Fm and Dundas Trough source lithologies used in this study.

Relative distribution plots show Kernel Density Estimates (KDE) and histograms for each lithology. KDEs were calculated with a fixed 20 Ma bandwidth and plots normalized to the height of each graph. Histograms are plotted with a 20 Ma bin sizes. The scale for each histogram is shown on the right-hand y-axis of each graph. Fill colors indicate distinct age ranges that represent natural groupings of Wynyard Fm detrital zircon dates. Vertical lines through the graphs highlight Wynyard Fm KDE peaks, dates of which are noted at the top of the graph. The lower plot shows the cumulative KDE for each lithology. Made using detritalPy v. 1.3.18 (Sharman et al., 2018). Descriptions of how each detrital zircon dataset was measured and how the data was processed are described in detail in the supplementary material section "Descriptions of West Tasmanian Source Lithologies." Data are available in File S1.

from the literature (Fig. 3; File S1; File S4). Preference was given to recently measured, high-n datasets.

The unmixing model was applied to DZ dates between 400 Ma and 2000 Ma. The older dates were excluded because they make up a very minor component of both the Wynyard Fm and source lithologies and were likely not accurately represented in source datasets with n < 300 (Pullen et al., 2014). Younger dates were excluded from the model because the only source for those dates is Devonian - Carboniferous granites (Hong et al., 2017; Kositcin & Everard, 2013) whose presence can be inferred without the use of a model (Fig. 3). Each model run consisted of 10,000 iterations where the distribution of dates from each potential source rock were randomly weighted so that the weights were summed to 100%. The weighted distributions were summed together as a cumulative distribution function (CDF) and a kernel density estimate (KDE). The resulting artificial mixtures of DZ dates were then compared to the Wynyard Fm using three methods:

1. two-sample K-S test D statistic (compares CDFs, zero is unity),
2. two-sample Kuiper test V statistic (compares CDFs, zero is unity), and
3. the cross-correlation coefficient (R^2, compares KDEs, one is unity).

The 100 best-fit models (top 1%) from each comparison method were retained and are shown in Fig. 4.

Four versions of the model were run, comparing the Wynyard Fm DZ dates with source lithologies that occur within 25 km, 50 km, 75 km, and 100 km of the Wynyard Fm site (Fig. 1, Fig. 4, Fig. 5). Sources within 25 km include the Arthur Metamorphic Complex (Mulder et al., 2020), Oonah Fm (Cumming et al., 2016; Mulder et al., 2018), and Owen Group (Habib et al., 2022). The 50 km model added the Upper and Lower Luina Gp (Cumming et al., 2016), the Mount Read Volcanics (Berry et al., 2001; Black et al., 1997; Mortensen et al., 2015) and Gordon Group (Habib et al., 2022), the 75 km model added the Wings Sandstone (Mulder et al., 2020), and the 100 km model added the Crimson Creek Fm (Mulder et al., 2020) and Success Creek Gp (Mulder et al., 2020).

Zircon population comparisons

The DZMix models were able to account for all DZ dates in the Wynyard Fm using source lithologies within 50 km, 75 km, and 100 km of the Wynyard Fm site (Fig. 1B, Fig. 4). The 25 km model was not able to account for all Wynyard Fm DZ dates (Fig. 5A; Fig. 4; Fig. 1B). All three of the successful DZMix model runs have overlapping mean fit parameter values (V, D, and R^2), indicating that none of these model runs are a better fit than the others (Fig. 5A; File S4). The successful DZMix models all identified both the Upper and Lower Luina Gps as the principal sources for the Wynyard Fm DZ (Fig. 5B-D), whereas the unsuccessful model (25 km) does not include the Luina Group. Other Dundas Trough sources, such as those included in the 25 km model, are needed to account for DZ dates found in the Wynyard Fm but not found in the Luina Gp (Fig. 4, Fig. 5). Presently,

the closest occurrence of the Luina Gp to the Wynyard Fm sample location along a paleo-flowpath is approximately 33 km (Fig. 1). Facies of the Upper and Lower Luina Gp that were sampled for zircons by Cumming et al. (2016) are present in the occurrence of the Luina Fm 33 km south of the Wynyard Fm site (Calver et al., 2011). Therefore, the model results indicate that all of the sampled Wynyard Fm DZs could have been sourced from the Dundas Trough within 33 km of the Wynyard Fm depositional site.

Though the three successful models (at 50 km, 75 km, and 100 km) were able to account for the presence of all Wynyard Fm DZ dates (Fig. 3; Fig. 4), none of the models produced a perfect fit for the Wynyard Fm. That is, the proportional abundances of the modeled dates did not match those measured in the Wynyard Fm zircons (Fig. 4). These misfits are likely due to both natural variability in source rocks and biases of the DZMix model. Some of the 'misfit' between DZ populations measured in the Wynyard Fm and the successfully modeled DZ populations likely occurred because the relative abundance of DZ dates in the combined source populations used for this study (Fig. 3) does not reflect the natural variability of these populations throughout the Dundas Trough. In other words, individual samples from potential source lithologies used in the model may not represent all the DZ dates or all possible mixtures of DZ dates within that formation. Additionally, some of this misfit between the Wynyard Fm DZ population and the modeled populations is due to the offset between DZ "date peaks" between the Wynyard Fm and Dundas Trough sources. The best example of this type of misfit is the Upper Luina Gp, which is likely an important source of Wynyard Fm zircons (see discussion in previous paragraph; Fig. 5). Though the CDFs of the Wynyard Fm and Upper Luina Gp are very similar, the Upper Luina Gp has two significant zircon populations with date peaks around 600 Ma and 1100 Ma that are not peaks in the Wynyard Fm (Fig. 3). However, both of those peaks in the Upper Luina Gp are part significant date populations in the Wynyard Fm with peaks centered on 660 Ma and 1035 Ma. This type of misfit between the Wynyard Fm DZ population and the modeled results likely occurred because the comparison methods in the DZMix model does not try to match age peaks, but instead favors DZ sources that are able to account for the most Wynyard Fm DZ dates.

Implications for the "Wynyard glacier"

The ultimate purpose of provenance work in glacigenic deposits is to re-construct the character of past glaciers. Prior work on the physical sedimentology of the Wynyard Fm has suggested that the Wynyard glacier:

1. flowed generally from south to north through the Dundas Trough (Fig. 1A; Hand, 1993),
2. had a warm (temperate) thermal regime (Henry et al., 2012; Ives, 2021; Powell, 1990), and
3. was part of, possibly an outlet glacier or ice stream of, a larger ice sheet that was centered over North Victoria Land (e.g., Ives, 2021; Veevers, 2006; Zurli et al., 2022).
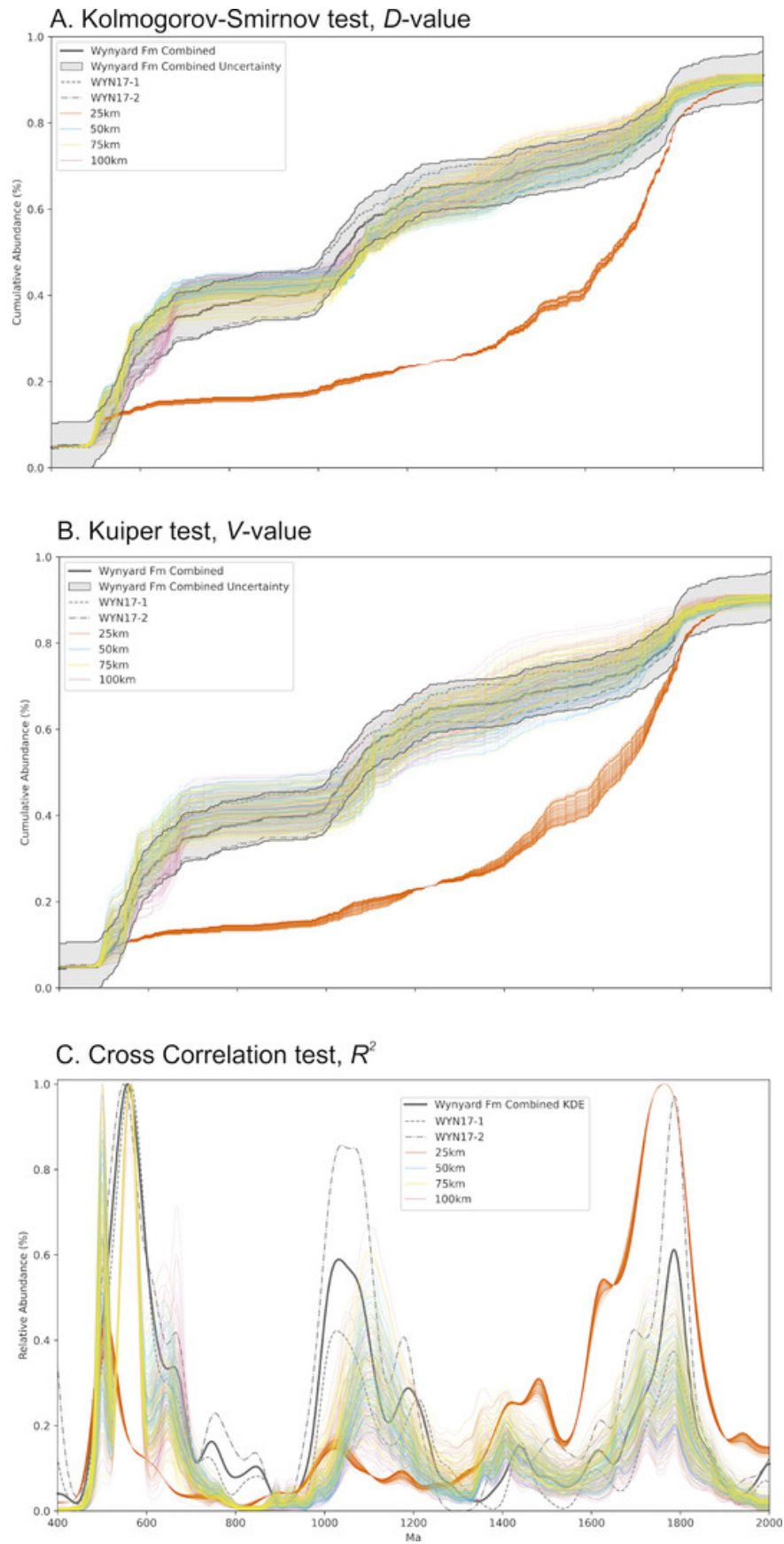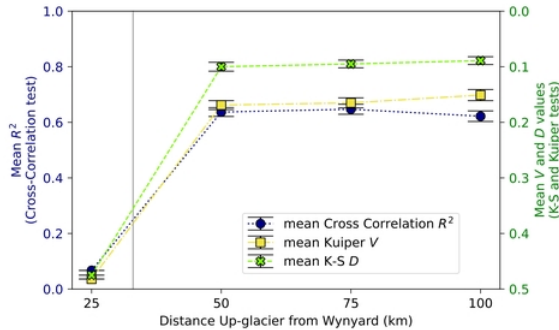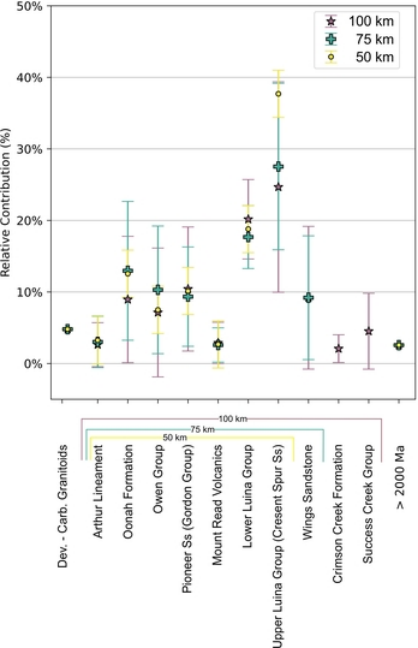
Figure 4. DZMix Model Results.

The Cumulative Distribution Functions (CDFs) and Kernel Density Estimate (KDE) graphs show the 100 best-fit (top 1%) A. K-S test D statistic comparison results, B. Kuiper test V statistic comparison results, and C. cross correlation (R2) comparison results. In all parts of the figure, grey lines and areas show the Wynyard Fm date distributions from this study, oranges lines are the results of the 25 km model run, blue lines are the results of the 50 km model run, yellow lines are the results of the 75 km model run, and purple lines are the results from the 100 km model run. Lines showing model results are transparent so that overlapping lines appear denser.
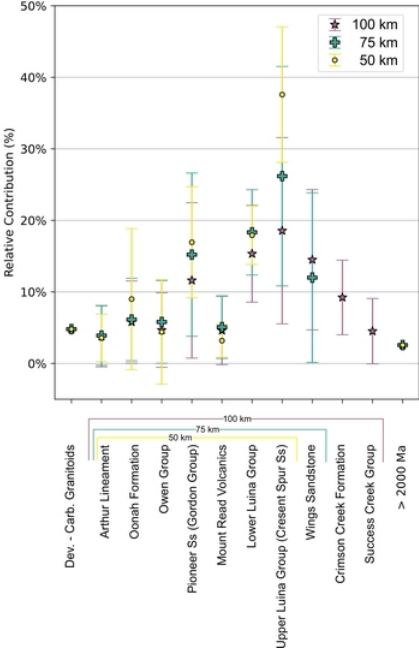
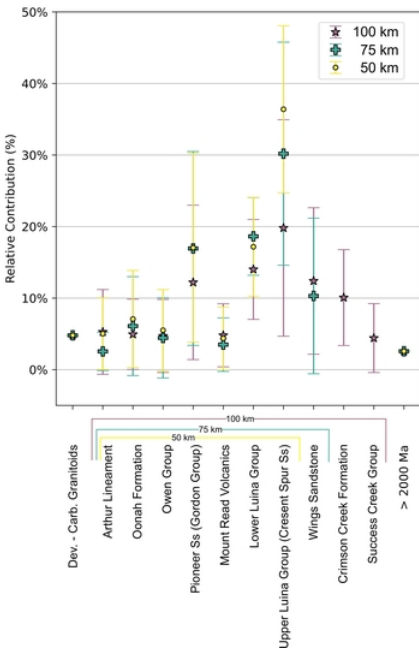**Figure 5. Mean fit parameters and predicted relative contribution results from the DZMix models.**

A. The mean fit parameter values for each model vs. distance from the Wynyard Fm sample site. Values towards the top of the plot indicate a better model fit. B. – D. The relative contribution of each detrital zircon potential source lithology in the Dundas Trough predicted by the successful 50 km, 75 km, and 100 km models. The point symbol shows the mean predicted contribution for each lithology in a model run based on the 100 (top 1%) best-fit modeled date distributions, and the error bars show the standard deviation of that mean. Relative contributions from Devonian – Carboniferous Granitoids (< 400 Ma) is 4.80% and zircons with dates > 2000 Ma is 2.57% for all modeled scenarios.

How then does the interpretation that Wynyard Fm DZ could have been sourced from Dundas Trough within ~33 km of the Wynyard Fm depositional site comport with these well-accepted sedimentological inferences?

First, the DZ date population of the Wynyard Fm supports the hypothesis that the Wynyard glacier flowed generally south to north through the Dundas Trough, due to both qualitative and mixing model comparisons showing that the DZ population of the studied Wynyard Fm samples could have been sourced from lithologies within the Dundas Trough.

Second, the interpretation that the subglacially-derived sediment of the Wynyard Fm was sourced from relatively proximal bedrock sources along the glacier's interpreted flow path is consistent with the Wynyard glacier having a warm thermal regime. All things being equal, in areas of the subglacial environment where subglacial erosion rates are high, local lithologies are most likely to dilute sediment provenance signals from more distal sources. Subglacial erosion rates are highest where glaciers have warm thermal regimes because those reaches of the glacier tend to have relative high sliding rates and high rates of subglacial meltwater discharge (e.g., Cook et al., 2020; Hallet et al., 1996). Beneath warm-based alpine glaciers, for which subglacial erosion is best studied, this behavior is typically confined to the glacier's ablation zone (Riihimaki et al., 2005). The margins of ice sheets may behave similarly to warm-based alpine glaciers in areas where surface meltwaters are able to reach the bed of the ice sheet (Cowton et al., 2012; Tuckett et al., 2019). Though subglacial sediment storage is poorly understood (e.g., Fernandez et al., 2016), in instances where a glacier is not actively over-riding pre-existing, unlithified sediments (e.g., Cowan et al., 2010; Hallet et al., 1996; Jaeger & Koppes, 2016; Motyka & Beget, 1996), many reports on subglacial erosion have effectively used the assumption that subglacial sediment storage is likely negligible compared to the volume of sediment produced from subglacially eroded bedrock over the same time scales (see discussions in Fernandez et al. (2016), Hogan et al. (2020), and Alley et al. (2019)). The implication being that most subglacially-created sediments are transported out of the subglacial system at a similar rate to which they are produced. Subglacial sediment flux likely occurs at similar rates to sediment efflux from the glacier margin, and is therefore likely act to bias the provenance of glacigenic sediments deposited at or near the margin of warm-based glaciers toward bedrock sources that underlie areas of high sliding speeds and high subglacial water flux near glacier margins. The interpretation of a warm-based thermal regime for the Wynyard glacier is therefore consistent with a "local" DZ provenance signal, since warm-based glaciers will preferentially erode and transport bedrock materials at high rates from proximal areas upglacier of the ice margin.

Third, the interpretation of a proximally-derived provenance for the Wynyard Fm DZ does not conflict with the idea that the Wynyard glacier was part of an ice sheet centered in Antarctica. While glaciers, especially those that span significant distances, are capable of transporting sediments hundreds of kilometers, most subglacially-derived sediment is deposited within 100 km of its bedrock source. This effect is likely to be amplified where glaciers have high sliding speeds and erosion rates, because the sediment flux rate through the subglacial system will be elevated. As mentioned in the previous paragraph, such conditions can exist in glaciers of all sizes, including portions of ice sheets (e.g., Chu et al., 2018). These conditions are especially likely at ice sheet margins (Cowton et al., 2012), which was likely the depositional setting for the Wynyard Fm. Therefore, glacier conditions that would bias the provenance of subglacially-derived sediment toward proximal sources can occur within large ice sheets. Indeed, much of the work that has shown this bias toward local sources has been done on sediments produced by the Pleistocene Laurentide and Fennoscandinavian ice sheets (e.g., Kujansuu & Saarnisto, 1990). Future glacial provenance studies may consider that a proximal provenance signal does not necessarily indicate a relatively small glacier, especially if the sedimentology indicates conditions associated with high erosions rates, such as a warm-based thermal regime and/or high meltwater discharge.

Towards a "local first" approach

The mechanics of glacier erosion and transport make it more likely that glacigenic sediments, on average, are derived from proximal (tens of kilometers) rather than distal (> 100 km) bedrock sources (e.g., Clark, 1987; Hooke et al., 2013; Larson & Mooers, 2008; Salonen, 1986). These mechanisms need to be considered in the characterization of glacigenic sediment provenance. Where constraints on glacier size and flow paths are limited, like in ancient glacial systems, a conservative approach to provenance should be taken where local lithologies are considered as potential sources before distal sources. This approach can also be used to identify non-local DZ sources through a process of elimination. If provenance indicators cannot be attributed to proximal sources, then progressively more distal sources should be considered. Shared distal sources between disparate glacial deposits of similar age may then be used to reconstruct past ice sheets.

A local first approach may be challenging in regions where DZ data for potential sources are often not available. This study was possible in Tasmania because of the abundance of high-quality, high-n DZ measurements from many of the potential source lithologies and the detailed study of the Permo-Carboniferous glaciation in Tasmania. In those cases, mixing models may not be appropriate except to help identify zircon populations missing from the source rock dataset. Future DZ studies could address this challenge by including the measurement of zircon dates in unmeasured, potential source lithologies.

Despite the challenges, approaching glacigenic sediment provenance in this way has the potential to deepen our understanding of ancient icehouse intervals like the Permo-Carboniferous. The rich literature on sediment transport and provenance in Holocene and late Pleistocene glacial systems makes it clear that considering local sources before distal sources is the prudent approach (e.g., Licht & Hemming, 2017; Salonen, 1986). As we begin to understand

the extent to which glaciations in the distant past were asynchronous and dynamic, this more nuanced basis for interpreting sedimentary provenance, and particularly DZ geochronology, may help in teasing out their complex histories.

,,,

Data Availability

The U-Pb measurements, interpreted dates, and geologic sample information for zircon data used in this study are available in the attached supplementary data. In case the attached resources are not available, information on the Wynyard Fm samples can be found under IGSN numbers IELRWWYN1 (WYN17-1) and IELRWWYN2 (WYN17-2) and U-Pb measurements of these samples have been uploaded to the Geochron database (www.geochron.org).

References

Alley, R. B., Cuffey, K. M., & Zoet, L. K. (2019). Glacial erosion: Status and outlook. *Annals of Glaciology*, *60*(80), 1–13. https://doi.org/10.1017/aog.2019.38

Andersen, T., Kristofferson, M., & Elburg, M. A. (2016). How far can we trust provenance and crustal evolution information from detrital zircons? A South African case study. *Gondwana Research*, *34*, 129–148. https://doi.org/10.1016/j.gr.2016.03.003

Andrews, J. T., & Fulton, R. J. (1987). Inception, growth, and decay of the Laurentide Ice Sheet. *Episodes, Journal of International Geoscience*, *10*(1), 13–15. https://doi.org/10.18814/epiiugs/1987/v10i1/006

Andrews, J. T., & MacLean, B. (2003). Hudson Strait ice streams: A review of stratigraphy, chronology and links with North Atlantic Heinrich events. *Boreas*, *32*(1), 4–17. https://doi.org/10.1080/03009480310001010

Andrews, J. T., Stavers, J. A., & Miller, G. H. (1985). Patterns of glacial erosion and deposition around Cumberland Sound, Frobisher Bay and Hudson Strait, and the location of ice streams in the Eastern Canadian Arctic. In M. J. Woldenberg (Ed.), *Models in Geomorphology: Binghamton Geomorphology Symposium 14* (pp. 93–118). Routledge. https://doi.org/10.4324/9780429260476

Banks, M. R. (1981). Late Paleozoic tillites of Tasmania. In M. J. Hambrey & W. B. Harland (Eds.), *Earth's Pre-Pleistocene Glacial Record* (pp. 495–501). Cambridge University Press.

Berry, R. F., Jenner, G. A., Meffre, S., & Tubrett, M. N. (2001). A North American provenance for Neoproterozoic to Cambrian sandstones in Tasmania? *Earth and Planetary Science Letters*, *192*(2), 207–222. https://doi.org/10.1016/s0012-821x(01)00436-8

Black, L. P., Everard, J. L., McClenaghan, M. P., Korsch, R. J., Calver, C. R., Fioretti, A. M., Brown, A. V., & Foudoulis, C. (2010). Controls on Devonian–Carboniferous magmatism in Tasmania, based on inherited zircon age patterns, Sr, Nd and Pb isotopes, and major and trace element geochemistry. *Australian Journal of Earth Sciences*, *57*(7), 933–968. https://doi.org/10.1080/08120099.2010.509407

Black, L. P., Kamo, S. L., Allen, C. M., Davis, D. W., Aleinikoff, J. N., Valley, J. W., Mundil, R., Campbell, I. H., Korsch, R. J., Williams, I. S., & Foudoulis, C. (2004). Improved 206Pb/238U microprobe geochronology by the monitoring of a trace-element-related matrix effect; SHRIMP, ID–TIMS, ELA–ICP–MS and oxygen isotope documentation for a series of zircon standards. *Chemical Geology*, *205*(1–2), 115–140. https://doi.org/10.1016/j.chemgeo.2004.01.003

Black, L. P., McClenaghan, M. P., Korsch, R. J., Everard, J. L., & Foudoulis, C. (2005). Significance of Devonian–Carboniferous igneous activity in Tasmania as derived from U–Pb SHRIMP dating of zircon. *Australian Journal of Earth Sciences*, *52*(6), 807–829. https://doi.org/10.1080/08120090500304232

Black, L. P., Seymour, D. B., Corbett, K. D., Cox, S. E., Streit, J. E., Bottrill, C. R., Calver, C. R., Everard, J. L., Green, G. R., McClenaghan, M. P., Pemberton, J., Taheri, J., & Turner, N. J. (1997). Dating Tasmania's Oldest Geological Events. *Australian Geological Survey Organisation Record*, *15*, 57.

Calver, C. R., Corbett, K. D., Cumming, G. V., Everard, J. L., Goscombe, B. D., Pemberton, J., Seymour, D. B., & Vicary, M. J. (2011). Geology of Northwest Tasmania. In *Mineral Resources Tasmania, Digital Geological Atlas 1:250 000 Scale Series, compilation, 1: 250 000, version 9, edition 2019.1.*

Chu, W., Schroeder, D. M., Seroussi, H., Creyts, T. T., & Bell, R. E. (2018). Complex basal thermal transition near the onset of Petermann Glacier, Greenland. *Journal of Geophysical Research: Earth Surface*, *123*(5), 985–995. https://doi.org/10.1029/2017JF004561

Clark, P. U. (1987). Subglacial sediment dispersal and till composition. *The Journal of Geology*, *95*(4), 527–541. https://doi.org/10.1086/629147

Clarke, M. J., & Forsyth, S. M. (1989). Late Carboniferous-Triassic. In C. F. Burrett & E. L. Martin (Eds.), *Geology and Mineral Resources of Tasmania, Geological Society of Australia Special Publication* (Vol. 15, pp. 293–338).

Cook, S. J., Swift, D. A., Kirkbride, M. P., Knight, P. G., & Waller, R. I. (2020). The empirical basis for modelling glacial erosion rates. *Nature Communications*, *11*(1), 759. https://doi.org/10.1038/s41467-020-14583-8

Cowan, E. A., Seramur, K. C., Powell, R. D., Willems, B. A., Gulick, S. P., & Jaeger, J. M. (2010). Fjords as temporary sediment traps: History of glacial erosion and deposition in Muir Inlet, Glacier Bay National Park, southeastern Alaska. *Geological Society of America Bulletin*, *122*(7–8), 1067–1080. https://doi.org/10.1130/B26595.1

Cowton, T., Nienow, P., Bartholomew, I., Sole, A., & Mair, D. (2012). Rapid erosion beneath the Greenland ice sheet. *Geology*, *40*(4), 343–346. https://doi.org/10.1130/g32687.1

Craddock, J. P., Ojakangas, R. W., Malone, D. H., Konstantinou, A., Mory, A. J., Bauer, W., Thomas, R. J., Affinati, S. C., Pauls, K. N., Zimmerman, U., Botha, G., Rochas-Campos, A., dos Santos, P. R., Tohver, E., Riccomini, C., Martin, J., Redfern, J., Horstwood, M., & Gehrels, G. (2019). Detrital zircon provenance of Permo-Carboniferous glacial diamictites across Gondwana. *Earth-Science Reviews*, *192*, 285–316. https://doi.org/10.1016/j.earscirev.2019.01.014

Cumming, G. V., Everard, J. L., & Meffre, S. (2016). *Age constraints and provenance of the Mount Bischoff inlier and the Luina Group: Evidence from LA-ICPMS U-Pb dating of detrital zircon* (No. Tasmanian Geological Survey Record UR2016/04). Mineral Resources Tasmania.

Elliot, D. H. (2013). The geological and tectonic evolution of the Transantarctic Mountains: A review. In M. J. Hambrey, P. F. Barker, P. J. Barrett, V. Bowman, B. Davies, J. L. Smellie, & M. Tranter (Eds.), *Antarctic Paleoenvironments and Earth-Surface Processes* (pp. 7–35). Geological Society of London, Special Publications 381. https://doi.org/10.1144/SP381.14

Fernandez, R. A., Anderson, J. B., Wellner, J. S., Minzoni, R. L., Hallet, B., & Smith, R. T. (2016). Latitudinal variation in glacial erosion rates from Patagonia and the Antarctic Peninsula (46°S–65°S). *Geological Society of America Bulletin*, *128*(5–6), 1000–1023. https://doi.org/10.1130/b31321.1

Gehrels, G. E. (2000). Introduction to detrital zircon studies of Paleozoic and Triassic strata in western Nevada and northern California. In M. J. Soreghan & G. E. Gehrels (Eds.), *Paleozoic and Triassic paleogeography and tectonics of western Nevada and Northern California* (pp. 1–18). Geological Society of America Special Paper 347. https://doi.org/10.1130/0-8137-2347-7.1

Gehrels, G. E., & Pecha, M. (2014). Detrital zircon U-Pb geochronology and Hf isotope geochemistry of Paleozoic and Triassic passive margin strata of western North America. *Geosphere*, *10*(1), 49–65. https://doi.org/10.1130/ges00889.1

Gehrels, G. E., Valencia, V. A., & Ruiz, J. (2008). Enhanced precision, accuracy, efficiency, and spatial resolution of U-Pb ages by laser ablation-multicollector-inductively coupled plasma-mass spectrometry. *Geochemistry, Geophysics, Geosystems*, *9*(3), Q03017. https://doi.org/10.1029/2007gc001805

Green, D. C., Brown, A. V., Calver, C. R., Corbett, K. D., Everard, J. L., Forsyth, S. M., Green, G., Goscombe, B. D., Woolward, I., Clark, M. J., McClenaghan, M. P., Vicary, M. J., Pemberton, J., Seymour, D. B., & Worthing, M. (2012). *Geology of Tasmania: Mineral Resources Tasmania, scale 1:500 000* [Graphic].

Griffis, N. P., Montañez, I. P., Fedorchuk, N., Isbell, J., Mundil, R., Vesely, F., Weinshultz, L., Iannuzzi, R., Gulbranson, E., Taboada, A., Pagani, A., Sanborn, M. E., Huyskens, M., Wimpenny, J., Linol, B., & Yin, Q.-Z. (2019). Isotopes to ice: Constraining provenance of glacial deposits and ice centers in west-central Gondwana. *Palaeogeography, Palaeoclimatology, Palaeoecology*, *531*, 108745. https://doi.org/10.1016/j.palaeo.2018.04.020

Habib, U., Meffre, S., Berry, R., & Kultaksayos, S. (2022). Detrital zircon ages, provenance and tectonic evolution in the early Paleozoic of Tasmania and Waratah Bay, Victoria. *Australian Journal of Earth Sciences*, *69*(5), 650–665. https://doi.org/10.1080/08120099.2022.2000493

Hallet, B., Hunter, L., & Bogen, J. (1996). Rates of erosion and sediment evacuation by glaciers: A review of field data and their implications. *Global and Planetary Change*, *12*(1–4), 213–235. https://doi.org/10.1016/0921-8181(95)00021-6

Hand, S. J. (1993). Palaeogeography of Tasmania's Permo-Carboniferous glacigenic sediments. In R. H. Findlay, R. Unrug, M. R. Banks, & J. J. Veevers (Eds.), *Gondwana Eight: Assembly, evolution and dispersal* (pp. 459–469). A.A. Balkema.

Henry, L. C., Isbell, J. L., Fielding, C. R., Domack, E. W., Frank, T. D., & Fraiser, M. L. (2012). Proglacial deposition and deformation in the Upper Carboniferous to Lower Permian Wynyard Formation, Tasmania: A process analysis. *Palaeogeography, Palaeoclimatology, Palaeoecology*, *315–316*, 142–157. https://doi.org/10.1016/j.palaeo.2011.11.020

Hogan, K. A., Jakobsson, M., Mayer, L., Reilly, B. T., Jennings, A. E., Stoner, J. S., Nielsen, T., Andresen, K. J., Nørmark, E., Heirman, K. A., Kamla, E., Jerram, K., Stranne, C., & Mix, A. (2020). Glacial sedimentation, fluxes and erosion rates associated with ice retreat in Petermann Fjord and Nares Strait, north-west Greenland. *The Cryosphere*, *14*(1), 261–286. https://doi.org/10.5194/tc-14-261-2020

Hong, W., Cooke, D. R., Huston, D. L., Maas, R., Meffre, S., Thompson, J., Zhang, L., & Fox, N. (2017). Geochronological, geochemical and Pb isotopic compositions of Tasmanian granites (southeast Australia): Controls on petrogenesis, geodynamic evolution and tin mineralisation. *Gondwana Research*, *46*, 124–140. https://doi.org/10.1016/j.gr.2017.03.009

Hooke, R. LeB., Cummings, D. I., Lesemann, J.-E., & Sharpe, D. R. (2013). Genesis of dispersal plumes in till. *Canadian Journal of Earth Sciences*, *50*(8), 847–855. https://doi.org/10.1139/cjes-2013-0018

Isbell, J. L., Henry, L. C., Gulbranson, E. L., Limarino, C. O., Fraiser, M. L., Koch, Z. J., Ciccioli, P. L., & Dineen, A. A. (2012). Glacial paradoxes during the late Paleozoic ice age: Evaluating the equilibrium line altitude as a control on glaciation. *Gondwana Research*, *22*(1), 1–19. https://doi.org/10.1016/j.gr.2011.11.005

Ives, L. R. W. (2021). Chapter 3: Contrasting styles of glacial sedimentation and glacier thermal regimes in the lower Wynyard Formation (Pennsylvanian – early Permian, Tasmanian Basin). In *A South Polar View of Late Paleozoic Glaciation: Physical Sedimentology and Provenance of Glacial Successions in the Tasmanian and Transantarctic Basins* (pp. 86–179). University of Wisconsin – Milwaukee, Dissertation. https://dc.uwm.edu/etd/2793

Jaeger, J. M., & Koppes, M. N. (2016). The role of the cryosphere in source-to-sink systems. *Earth-Science Reviews*, *v. 153*, 43–76. https://doi.org/10.1016/j.earscirev.2015.09.011

Kositcin, N., & Everard, J. L. (2013). *New SHRIMP U–Pb zircon ages from Tasmania: July 2012–June 2013* (No. Geoscience Australia Record 2013/22, Tasmanian Geological Survey Record 2013/02). Geoscience Australia.

Kujansuu, R., & Saarnisto, M. (Eds.). (1990). *Glacial indicator tracing*. Balkema. https://doi.org/10.1201/9781003079415

Larson, P. C., & Mooers, H. D. (2008). Glacial indicator dispersal processes: A conceptual model. *Boreas*, *33*(3), 238–249. https://doi.org/10.1111/j.1502-3885.2004.tb01144.x

Lawton, T. F., Blakey, R. C., Stockli, D. F., & Liu, L. (2021). Late Paleozoic (Late Mississippian–Middle Permian) sediment provenance and dispersal in western equatorial Pangea. *Palaeogeography, Palaeoclimatology, Palaeoecology*, *572*, 110386. https://doi.org/10.1016/j.palaeo.2021.110386

Licht, K. J., & Hemming, S. R. (2017). Analysis of Antarctic glacigenic sediment provenance through geochemical and petrologic applications. *Quaternary Science Reviews*, *164*, 1–24. https://doi.org/10.1016/j.quascirev.2017.03.009

Lønne, I. (1995). Sedimentary facies and depositional architecture of ice-contact glaciomarine systems. *Sedimentary Geology*, *98*(1–4), 13–43. https://doi.org/10.1016/0037-0738(95)00025-4

Martin, J. R., Redfern, J., Horstwood, M. S. A., Mory, A. J., & Williams, B. P. J. (2019). Detrital zircon age and provenance constraints on late Paleozoic ice-sheet growth and dynamics in Western and Central Australia. *Australian Journal of Earth Sciences*, *66*(2), 183–207. https://doi.org/10.1080/08120099.2019.1531925

Mortensen, J. K., Gemmell, J. B., McNeill, A. W., & Friedman, R. M. (2015). High-Precision U-Pb zircon Chronostratigraphy of the Mount Read Volcanic Belt in Western Tasmania, Australia: Implications for VHMS Deposit Formation. *Economic Geology*, *110*(2), 445–468. https://doi.org/10.2113/econgeo.110.2.445

Motyka, R. J., & Beget, J. E. (1996). Taku Glacier, southeast Alaska, USA: Late Holocene history of a tidewater glacier. *Arctic and Alpine Research*, *28*(1), 42–51. https://doi.org/10.2307/1552084

Mulder, J. A., Berry, R. F., Halpin, J. A., Meffre, S., & Everard, J. L. (2018). Depositional age and correlation of the Oonah Formation: Refining the timing of Neoproterozoic basin formation in Tasmania. *Australian Journal of Earth Sciences*, *65*(3), 391–407. https://doi.org/10.1080/08120099.2018.1426629

Mulder, J. A., Everard, J. L., Cumming, G., Meffre, S., Bottrill, R. S., Merdith, A. S., Halpin, J. A., McNeill, A. W., & Cawood, P. A. (2020). Neoproterozoic opening of the Pacific Ocean recorded by multi-stage rifting in Tasmania, Australia. *Earth-Science Reviews*, *201*, 103041. https://doi.org/10.1016/j.earscirev.2019.103041

Mulder, J. A., Halpin, J. A., & Daczko, N. R. (2015). Mesoproterozoic Tasmania: Witness to the East Antarctica–Laurentia connection within Nuna. *Geology*, *43*(9), 759–762. https://doi.org/10.1130/g36850.1

Paces, J. B., & Miller, J. D., Jr. (1993). Precise U-Pb ages of Duluth Complex and related mafic intrusions, northeastern Minnesota: Geochronological insights to physical, petrogenetic, paleomagnetic, and tectonomagmatic processes associated with the 1.1 Ga Midcontinent Rift System. *Journal of Geophysical Research: Solid Earth*, *98*(B8), 13997–14013. https://doi.org/10.1029/93jb01159

Powell, R. D. (1990). Glacimarine processes at grounding-line fans and their growth to ice-contact deltas. In J. A. Dowdeswell & J. D. Scourse (Eds.), *Glacimarine Environments: processes and sediments* (Vol. 53, pp. 53–73). Geological Society Special Publication. https://doi.org/10.1144/gsl.sp.1990.053.01.03

Pullen, A., Ibáñez-Mejia, M., Gehrels, G. E., Giesler, D., & Pecha, M. (2018). Optimization of a laser ablation-single collector-inductively coupled plasma-mass spectrometer (Thermo Element 2) for accurate, precise, and efficient zircon U-Th-Pb geochronology. *Geochemistry, Geophysics, Geosystems*, *19*(10), 3689–3705. https://doi.org/10.1029/2018gc007889

Pullen, A., Ibáñez-Mejía, M., Gehrels, G. E., Ibáñez-Mejía, J. C., & Pecha, M. (2014). What happens when n= 1000? Creating large-n geochronological datasets with LA-ICP-MS for geologic investigations. *Journal of Analytical Atomic Spectrometry*, *29*(6), 971–980. https://doi.org/10.1039/c4ja00024b

Reid, C. M., Forsyth, S. M., Clarke, M. J., & Bacon, C. A. (2014). Chapter 7. The Parmeener Supergroup—Late Carboniferous to Triassic. In K. D. Corbett, P. G. Quilty, & C. R. Calver (Eds.), *Geological Evolution of Tasmania, Geological Society of Australia Special Publications* (Vol. 24, pp. 363–384).

Riihimaki, C. A., MacGregor, K. R., Anderson, R. S., Anderson, S. P., & Loso, M. G. (2005). Sediment evacuation and glacial erosion rates at a small alpine glacier. *Journal of Geophysical Research: Earth Surface*, *110*(F3). https://doi.org/10.1029/2004jf000189

Salonen, V.-P. (1986). Glacial transport distance distributions of surface boulders in Finland. *Geological Survey of Finland, Bulletin*, *58*.

Sharman, G. R., Sharman, J. P., & Sylvester, Z. (2018). detritalPy: A Python-based toolset for visualizing and analysing detrital geo-thermochronologic data. *The Depositional Record*, *4*(2), 202–215. https://doi.org/10.1002/dep2.45

Sundell, K. E., & Saylor, J. E. (2017). Unmixing detrital geochronology age distributions. *Geochemistry, Geophysics, Geosystems*, *18*(8), 2872–2886. https://doi.org/10.1002/2016gc006774

Tuckett, P. A., Ely, J. C., Sole, A. J., Livingstone, S. J., Davison, B. J., Melchior van Wessem, J., & Howard, J. (2019). Rapid accelerations of Antarctic Peninsula outlet glaciers driven by surface melt. *Nature Communications*, *10*(1), 1–8. https://doi.org/10.1038/s41467-019-12039-2

Veevers, J. J. (2006). Updated Gondwana (Permian–Cretaceous) earth history of Australia. *Gondwana Research*, *9*(3), 231–260. https://doi.org/10.1016/j.gr.2005.11.005

Zotto, S. C., Moecher, D. P., Niemi, N. A., Thigpen, J. R., & Samson, S. D. (2020). Persistence of Grenvillian dominance in Laurentian detrital zircon age systematics explained by sedimentary recycling: Evidence from detrital zircon double dating and detrital monazite textures and geochronology. *Geology*, *48*(8), 792–797. https://doi.org/10.1130/g47530.1

Zurli, L., Cornamusini, G., Woo, J., Liberato, G. P., Han, S., Kim, Y., & Talarico, F. M. (2022). Detrital zircons from Late Paleozoic Ice Age sequences in Victoria Land (Antarctica): New constraints on the glaciation of southern Gondwana. *Geological Society of America Bulletin*, *134*(1–2), 160–178. https://doi.org/10.1130/b35905.1

Supplementary Materials

Supplemental Documatation

Download: https://thesedimentaryrecord.scholasticahq.com/article/38180-a-local-first-approach-to-glacigenic-sediment-provenance-demonstrated-using-u-pb-detrital-zircon-geochronology-of-the-permo-carboniferous-wynyard-fo/attachment/99318.docx

Figure S1

Download: https://thesedimentaryrecord.scholasticahq.com/article/38180-a-local-first-approach-to-glacigenic-sediment-provenance-demonstrated-using-u-pb-detrital-zircon-geochronology-of-the-permo-carboniferous-wynyard-fo/attachment/99955.jpg

Figure S2

Download: https://thesedimentaryrecord.scholasticahq.com/article/38180-a-local-first-approach-to-glacigenic-sediment-provenance-demonstrated-using-u-pb-detrital-zircon-geochronology-of-the-permo-carboniferous-wynyard-fo/attachment/99956.jpg

Figure S3

Download: https://thesedimentaryrecord.scholasticahq.com/article/38180-a-local-first-approach-to-glacigenic-sediment-provenance-demonstrated-using-u-pb-detrital-zircon-geochronology-of-the-permo-carboniferous-wynyard-fo/attachment/99957.jpg

Figure S4

Download: https://thesedimentaryrecord.scholasticahq.com/article/38180-a-local-first-approach-to-glacigenic-sediment-provenance-demonstrated-using-u-pb-detrital-zircon-geochronology-of-the-permo-carboniferous-wynyard-fo/attachment/99958.jpg

Figure S5

Download: https://thesedimentaryrecord.scholasticahq.com/article/38180-a-local-first-approach-to-glacigenic-sediment-provenance-demonstrated-using-u-pb-detrital-zircon-geochronology-of-the-permo-carboniferous-wynyard-fo/attachment/99960.jpg

Figure S6

Download: https://thesedimentaryrecord.scholasticahq.com/article/38180-a-local-first-approach-to-glacigenic-sediment-provenance-demonstrated-using-u-pb-detrital-zircon-geochronology-of-the-permo-carboniferous-wynyard-fo/attachment/99961.jpg

File S1

Download: https://"thesedimentaryrecord.scholasticahq.com/article/38180-a-local-first-approach-to-glacigenic-sediment-provenance-demonstrated-using-u-pb-detrital-zircon-geochronology-of-the-permo-carboniferous-wynyard-fo/attachment/99963.xlsx

File S2

Download: https://thesedimentaryrecord.scholasticahq.com/article/38180-a-local-first-approach-to-glacigenic-sediment-provenance-demonstrated-using-u-pb-detrital-zircon-geochronology-of-the-permo-carboniferous-wynyard-fo/attachment/99964.xlsx

File S3

Download: https://thesedimentaryrecord.scholasticahq.com/article/38180-a-local-first-approach-to-glacigenic-sediment-provenance-demonstrated-using-u-pb-detrital-zircon-geochronology-of-the-permo-carboniferous-wynyard-fo/attachment/99965.xlsx

File S4

Download: https://thesedimentaryrecord.scholasticahq.com/article/38180-a-local-first-approach-to-glacigenic-sediment-provenance-demonstrated-using-u-pb-detrital-zircon-geochronology-of-the-permo-carboniferous-wynyard-fo/attachment/99966.zip

File S5

Download: https://thesedimentaryrecord.scholasticahq.com/article/38180-a-local-first-approach-to-glacigenic-sediment-provenance-demonstrated-using-u-pb-detrital-zircon-geochronology-of-the-permo-carboniferous-wynyard-fo/attachment/99967.zip